

---

# Nonlinear Oscillators at Our Fingertips

---

Tanya Leise and Andrew Cohen

---

**1. AN EXPERIMENT WITH COUPLED OSCILLATORS.** We begin with an experiment that requires minimal equipment: you just need your left and right forefingers. To get warmed up, first point your right forefinger in the natural way (we refer to this position as the “equilibrium position”). Next move your right forefinger back and forth in a motion that could be graphed as shown in Figure 1, where the displacement of the fingertip equals the distance from the equilibrium position.

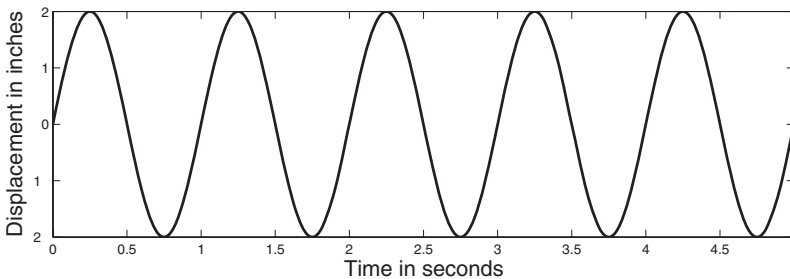


**Figure 1.** Oscillation  $x(t) = 2 \cos(2\pi t - \pi/2)$  of a single finger with a frequency  $\omega = 2\pi$  (yielding one cycle per second), amplitude  $r = 2$ , and phase angle  $\phi = -\pi/2$ .

Continue oscillating your right forefinger and begin oscillating your left forefinger (it may be helpful to point your fingers at each other and anchor your wrists; only the fingers should move, not your hands). Unless you are a drummer, your fingers will tend to naturally fall into one of two relative motions. The motion that is generally the most comfortable is to move the fingers in unison, as though one were a mirror image of the other. We refer to this as “in-phase” oscillation, and the graphs of the left and right finger motions are identical. The other natural motion is to move the fingers opposite each other, so that they pass each other at the equilibrium point going in opposite directions. We refer to this as “antiphase” oscillation, and the graphs of the left and right finger motions resemble those in Figure 2.

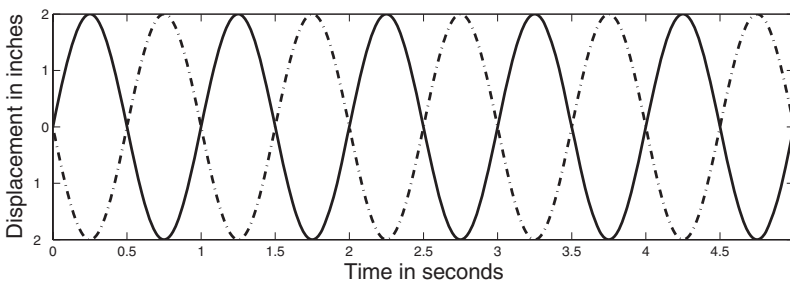


**Figure 2.** Antiphase oscillation of the two fingers at a frequency of one cycle per second, where the solid line represents the right finger  $x_R(t) = 2 \cos(2\pi t - \pi/2)$  and the dotted line the left finger  $x_L(t) = 2 \cos(2\pi t + \pi/2)$ . (The phase difference is the difference between the phase angles:  $\Delta\phi = \pi/2 - (-\pi/2) = \pi$ .)

Now we're ready for the interesting part of this experiment (conceived by Kelso [11]). Start oscillating your fingers antiphase at a comfortable pace. Gradually speed up the motion, increasing the frequency until something interesting happens. You should experience a sudden "phase transition" from antiphase to in-phase motion. This transition tends to be abrupt; past a certain frequency, most people cannot oscillate their fingers opposite each other, although they can still oscillate them in unison. The graph of this experiment might look something like the caricature in Figure 3. A similar and even more intriguing experiment can be done with two people. Have each person swing one of their legs antiphase with the other person's leg (each person watches the other person's leg in order to coordinate the leg motions). Increase the frequency of the leg swinging, and you will witness the same phenomenon of the legs snapping into synchronous motion at a critical frequency [15]. Try it!

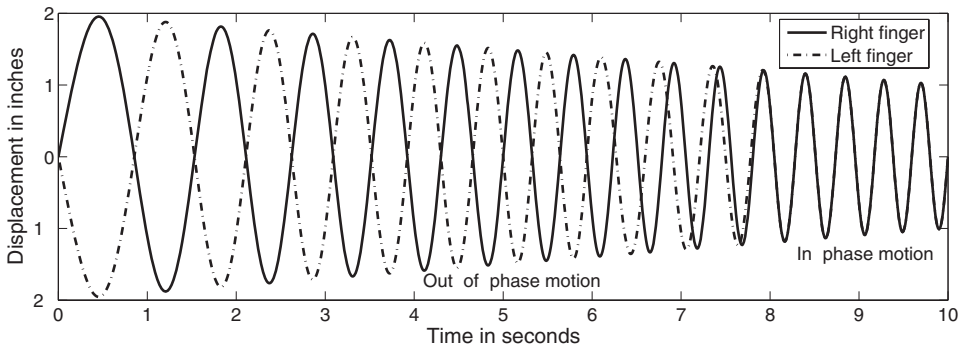


**Figure 3.** Caricature of the oscillations of two fingers as the frequency increases. The oscillations are initially antiphase with a frequency of one cycle per second. As the frequency increases past roughly 2 cycles per second, a transition occurs from antiphase to in-phase motion. Also observe that the amplitude of the oscillations decreases from 2 inches to 1 inch as the frequency increases from 1 cycle per second to more than 2 cycles per second. (These numbers are for illustrative purposes and don't correspond to actual experimental data.)

These experiments may be nice parlor tricks (and can liven up a modeling or differential equation course), but why bother studying such apparently inconsequential quirks in a serious way? The overarching goal in such research is to understand how coordination is achieved by our neuromuscular system, perhaps in conjunction with our perceptual system (a very difficult and nearly overwhelming task). Studying a relatively simple system that includes a few key features can be used as a stepping stone to eventually analyzing more important but very complex systems.

Our goal in this article is to explore a model of the "finger twiddling" phenomenon, noting the model's successes and shortcomings, and thereby to peek into the magical world of coupled nonlinear oscillators. We employ a different method of analysis than has previously been applied to this model, in order to reveal more clearly its strengths and weaknesses and to show how two forms of the model are related. This approach also has the advantage of being accessible to a general mathematical audience, including advanced undergraduate students in a differential equations or modeling course (The first author's students have found this material quite appealing and a nice change from the usual sorts of applied problems).

The model we examine was constructed by Haken, Kelso, and Bunz [9] (and so dubbed the HKB-model) two decades ago with the aim of discovering the necessary ingredients in a model to reproduce four basic features of Kelso's experimental results in the finger oscillations task:

1. Only two stable states exist: in-phase motion and antiphase motion.
2. As frequency increases, the amplitude of motion decreases, as shown in Figure 3.
3. As the frequency increases past a critical frequency, antiphase motion abruptly changes to in-phase motion.
4. Beyond this transition, only in-phase motion is possible. That is, for frequencies above the critical frequency, only in-phase motion is stable, while below the critical frequency both in-phase and antiphase motions are stable.

The general solution  $x(t) = r \cos(\omega t + \phi)$  represents the sort of periodic motion of interest for us, where  $r$  is the amplitude,  $\omega$  is the frequency, and  $\phi$  is the phase angle, as indicated in Figures 1 and 2. In section 2, we propose a differential equation model of a single finger that can (at least approximately) produce solutions of this form and also exhibits decreasing amplitude as the frequency increases. In section 3, we couple two of these differential equations and verify that all four desired experimental features emerge from the coupled system. The analytical method we employ was chosen because it paints a broader picture of the HKB-model's predictions than the methods used in [9], [10], or [13], and it reveals a mathematical connection between the differential equation form of the HKB-model given in section 3 and the potential function form discussed in section 4. In section 5, we reflect on this modeling effort and place it in a more general context.

We begin, as we began our first experiment, by considering the oscillation of a single finger.

**2. A SINGLE NONLINEAR OSCILLATOR.** The model for a single finger should both exhibit decreasing amplitude of oscillation as the frequency increases and have the potential for multiple stable states once it is coupled to another similar oscillator. A good starting place is to treat each finger as a mass connected to a spring in order to model the oscillations of “finger twiddling.” The simplest differential equation describing a mass-spring system is derived by combining Newton’s second law (force equals mass times acceleration) with Hooke’s law (the force required to stretch or compress a string is proportional to the displacement from equilibrium):

$$m\ddot{x} + kx = 0,$$

where  $m$  is the mass and  $k$  is the Hooke’s law constant. The natural frequency of this system is then  $\omega = \sqrt{k/m}$ , and once set in motion the mass-spring oscillates at this frequency forever, with the amplitude depending on the initial position and velocity. Hence this simplest mass-spring model cannot capture the complexity of behavior we are seeking.

To make the situation more realistic, a damping force should be added, where the damping increases as the speed increases (imagine trying to walk through water versus running through water). Because a linearly damped system returns to equilibrium, we need to add an external forcing term in order to obtain steady periodic motion:

$$m\ddot{x} + c\dot{x} + kx = F_e \cos \omega t,$$

where  $c$  is the damping coefficient and  $F_e \cos \omega t$  is the external force. This system simply oscillates (after a brief transient period) at the same frequency as the external force. Again, we need to add a further ingredient in order to obtain interesting behavior.

We must now consider the addition of a nonlinearity of some sort. We could add nonlinear damping terms, or we could generalize the forcing term to involve the displacement or velocity in a nonlinear manner. The HKB-model includes nonlinear

damping terms in order to obtain a natural mode of oscillation without a forcing term. Other modelers have made different choices (for example, see [4], which looks at adding perception to the model via the forcing term).

Well-studied differential equations with nonlinear damping terms include the Van der Pol equation

$$\ddot{x} - \alpha \dot{x} + \gamma x^2 \dot{x} + \omega^2 x = 0,$$

and the Rayleigh equation

$$\ddot{x} - \alpha \dot{x} + \beta \dot{x}^3 + \omega^2 x = 0.$$

Each system is self-sustaining, due to the minus sign in front of the linear “damping” term; once set in motion, the system stays in motion in the absence of external forces. However, the Van der Pol model does not fulfill the requirement that the amplitude of the oscillation decrease as the frequency  $\omega$  increases, and the Rayleigh model predicts unbounded amplitudes as the frequency decreases to zero. Fortunately, a combination of the two models fulfills our modeling goals. This choice was motivated by Kelso’s experimental findings, and its appropriateness is confirmed in [10], which shows that such a hybrid model fits data from subjects very well, while the Van der Pol and Rayleigh models by themselves do not.

Hence we consider the following hybrid of the Van der Pol and Rayleigh differential equations to model the position of a fingertip:

$$\ddot{x} - \alpha \dot{x} + \beta \dot{x}^3 + \gamma x^2 \dot{x} + \omega^2 x = 0, \quad (1)$$

where all coefficients are assumed to be positive. An oscillatory solution  $x(t)$  to the nonlinear equation (1) consists of a dominant term with frequency  $\omega$  plus other higher frequency terms of relatively small amplitude. Neglecting the higher frequency terms lead to the following approximate solution to (1):<sup>1</sup>

$$x(t) \approx \frac{2\sqrt{\alpha}}{\sqrt{\gamma + 3\beta\omega^2}} \cos(\omega t + \phi), \quad (2)$$

in which  $r = 2\sqrt{\alpha}/\sqrt{\gamma + 3\beta\omega^2}$  is the predicted amplitude of a finger oscillating with frequency  $\omega$ , and  $\phi$  is the phase angle (determined by initial conditions). The approximate solution (2) can be used to determine best-fit values for  $\alpha$ ,  $\beta$ , and  $\gamma$  based on single finger motion experiments with various values of  $\omega$ . (N.B. we assume that  $\alpha$ ,  $\beta$ , and  $\gamma$  are fixed parameters associated with a particular person’s finger, while  $\omega$  is a control parameter that can be varied in order to observe the system’s response.)

Now that we have a viable model for a single finger and an experimental means of determining parameter values for that model, we are ready to move on to the coupled system.

**3. COUPLED NONLINEAR OSCILLATORS.** To model the coordination between the two fingers, we must couple two of the hybrid oscillators (imagine coupling

---

<sup>1</sup>For the interested reader, the approximate solution can be derived fairly easily using what is sometimes referred to as the small parameter method of Poincaré as extended by Krylov-Bogoliubov, which also shows that the period of the true solution equals  $2\pi/\omega + O(\alpha^2)$  (see, for example, chapter 10 of [14] for a classical treatment).

two railway cars, so that the motion of one affects that of the other, although in our context the coupling will be very weak). This “coupling” can be accomplished by adding a term (“coupling function”) to the two differential equations representing the left and right fingers that describes the interaction between them. Determining an appropriate coupling function remains a very difficult open problem, so unfortunately there is little to guide us here. To be consistent with our approach for modeling a single finger’s oscillations, we again use a few odd-degree polynomial terms involving the displacement and the velocity, mimicking the damping terms in (1):  $-\alpha\dot{x} + \beta\dot{x}^3 + \gamma x^2\dot{x}$ . Because finger coordination focuses on the relative motion of the two fingers, it seems natural to replace the quantity  $x$  with the difference  $x_L - x_R$  between the left and right fingers, leading to a coupling function  $-a(\dot{x}_L - \dot{x}_R) + b(\dot{x}_L - \dot{x}_R)^3 + c(x_L - x_R)^2(\dot{x}_L - \dot{x}_R)$ . If we wish to oscillate in unison, then the differences  $\Delta x = x_L - x_R$  and  $\Delta v = \dot{x}_L - \dot{x}_R$  must be zero over the entire motion. If  $\Delta x$  and  $\Delta v$  are not quite zero, then the coupling function acts as a generalized forcing term that nudges the fingers toward synchronization. If we wish to oscillate in opposite directions, then  $\Delta x$  must be zero when  $\Delta v$  attains its maximum value, and vice versa. In essence, each type of coordination corresponds to a certain pattern in  $\Delta x$  and  $\Delta v$  that is quite distinctive, and if the motion is near a stable pattern of motion, then the coupling function nudges the system closer to that pattern.

Combining this coupling function with the differential equation (1) describing a single finger’s motion results in the following system of coupled nonlinear differential equations:

$$\ddot{x}_L - \dot{x}_L(\alpha - \beta\dot{x}_L^2 - \gamma x_L^2) + \omega^2 x_L = -(\dot{x}_L - \dot{x}_R)(a - b(\dot{x}_L - \dot{x}_R)^2 - c(x_L - x_R)^2), \quad (3)$$

$$\ddot{x}_R - \dot{x}_R(\alpha - \beta\dot{x}_R^2 - \gamma x_R^2) + \omega^2 x_R = -(\dot{x}_R - \dot{x}_L)(a - b(\dot{x}_R - \dot{x}_L)^2 - c(x_R - x_L)^2), \quad (4)$$

where all coefficients are assumed to be nonnegative and the coupling coefficients  $a$ ,  $b$ , and  $c$  are assumed to be “small” relative to  $\alpha$ ,  $\beta$ , and  $\gamma$ , yielding a weak coupling. This system is the HKB-model with the addition of the  $b(\dot{x}_L - \dot{x}_R)^3$  terms, which have been included here for purposes of showing how to determine which terms are necessary for modeling the phenomenon and which are superfluous.

We wish to determine the limit cycles (i.e., periodic solutions of (3)–(4)) of the coupled oscillators and ascertain whether each limit cycle is stable (also called attracting), in the sense that nearby trajectories approach the limit cycle. To gain some intuition about stable limit cycles, examine Figure 4. The slanted line segment in graph (a) is a limit cycle corresponding to in-phase motion: the displacements  $x_L$  and  $x_R$  remain equal, tracing a line segment over time from  $(-2, -2)$  to  $(2, 2)$ , back to  $(-2, -2)$ , and then repeating. The slanted line segment in graph (d) is a limit cycle corresponding to antiphase motion, tracing a line segment from  $(-2, 2)$  to  $(2, -2)$ , back to  $(-2, 2)$ , and then repeating. If a trajectory starts at a point near a stable limit cycle, then it follows a path that approaches the limit cycle, as seen in graphs (b) and (c) for in-phase motion and in graphs (e) and (f) for antiphase motion.

We are also interested in identifying changes in stability that occur as the frequency  $\omega$  increases (that is, we wish to verify that the model can indeed experience the desired phase transitions). We also wish to discover whether a weak coupling (i.e., “small” values of  $a$ ,  $b$ , and  $c$ ) can lead to the desired phase-switching behavior.

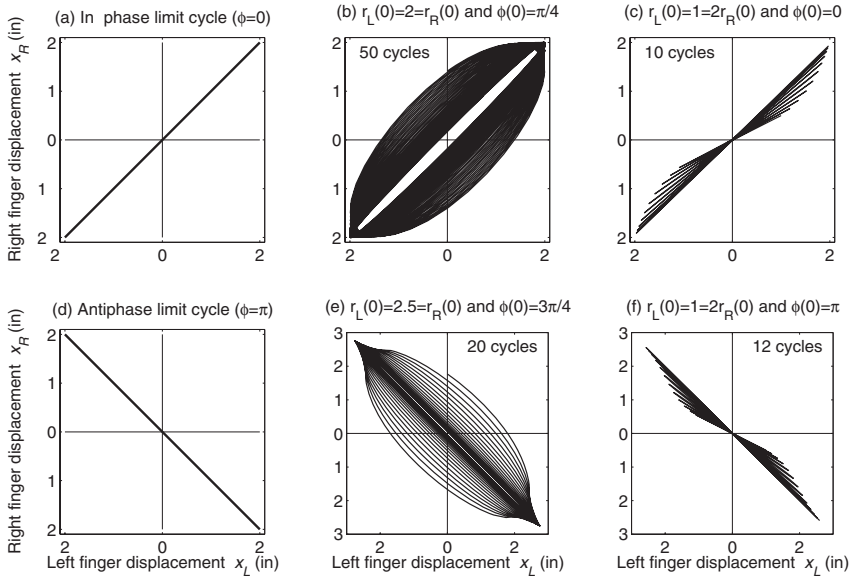


**Figure 4.** The limit cycle in graph (a) corresponds to both fingers oscillating as in Figure 1 and the limit cycle in (d) corresponds to the motion in Figure 2. The numerical solutions of (3)–(4) in graphs (b) and (c) converge to solution #2 in Table 1, while those in graphs (e) and (f) converge to #3. All four of these numerical solutions use parameters  $\alpha = 0.5$ ,  $\beta = 0.001$ ,  $\gamma = 0.38$ ,  $a = 0.05$ ,  $b = 0$ ,  $c = 0.036$ , and  $\omega = 2\pi$ .

We generalize our periodic solution for a single oscillator,  $x(t) = r \cos(\omega t + \phi)$ , by assuming nearly periodic solutions for each finger, solutions whose amplitudes and phase angles may change over time:

$$x_k(t) = r_k(t) \cos(\omega t + \phi_k(t)), \quad (5)$$

for  $k = L$  and  $k = R$ . A limit cycle has  $\dot{r}_k = 0$  and  $\dot{\phi}_k = 0$ , so we seek limit cycles by finding expressions for  $\dot{r}_k$  and  $\dot{\phi}_k$ , setting them equal to zero, and then solving for  $r_k$  and  $\phi_k$ .

We observe that if these oscillations are fairly steady (recalling that the coupling between the finger is assumed to be weak) with  $\dot{r}_k \approx 0$  and  $\dot{\phi}_k \approx 0$ , then the velocity obtained by differentiating (5) is approximately

$$\dot{x}_k(t) = -\omega r_k(t) \sin(\omega t + \phi_k(t)). \quad (6)$$

Of course, this ignores the time derivatives of  $r_k(t)$  and  $\phi_k(t)$ . Comparing (6) with the time derivative of (5) under the assumptions that  $\dot{r}_k \neq 0$  and  $\dot{\phi}_k \neq 0$ , we see that (6) is only true if

$$\dot{r}_k(t) \cos(\omega t + \phi_k(t)) - r_k(t) \dot{\phi}_k(t) \sin(\omega t + \phi_k(t)) = 0 \quad (k = L, R). \quad (7)$$

We have four equations in  $\dot{r}_L$ ,  $\dot{r}_R$ ,  $\dot{\phi}_L$ , and  $\dot{\phi}_R$  if we take the two equations given by (7), plus the two equations obtained by substituting (5) and (6) into (3) and (4), where the second derivatives are obtained by taking the derivative of (6). Solving these four equations for  $\dot{r}_L$ ,  $\dot{r}_R$ ,  $\dot{\phi}_L$ , and  $\dot{\phi}_R$  leads to rather complicated and unhelpful expressions that involve time in a complex manner (note that use of a computer algebra package

is extremely helpful for solving the four equations, as well as for other calculations done later—see [www.amherst.edu/~tleise](http://www.amherst.edu/~tleise) for a sample Mathematica file). Since we assume that these time derivatives change very little over one period  $2\pi/\omega$ , we can simplify their expressions by averaging over a period. This procedure leads to the following, where  $\Delta\phi = \phi_L - \phi_R$  is the phase difference between the hands:

$$\begin{aligned} \dot{r}_L(t) \approx \frac{\omega}{2\pi} \int_t^{t+2\pi/\omega} \dot{r}_L(\tau) d\tau &= \frac{1}{8} [r_R(4a - (c + 3b\omega^2)(3r_L^2 + r_R^2)) \cos \Delta\phi \\ &\quad + r_L(4(\alpha - a) + r_L^2(c - \gamma + 3(b - \beta)\omega^2) \\ &\quad + r_R^2(c + 3b\omega^2)(2 + \cos 2\Delta\phi))], \end{aligned} \tag{8}$$

$$\begin{aligned} \dot{r}_R(t) \approx \frac{\omega}{2\pi} \int_t^{t+2\pi/\omega} \dot{r}_R(\tau) d\tau &= \frac{1}{8} [r_L(4a - (c + 3b\omega^2)(3r_R^2 + r_L^2)) \cos \Delta\phi \\ &\quad + r_R(4(\alpha - a) + r_R^2(c - \gamma + 3(b - \beta)\omega^2) \\ &\quad + r_L^2(c + 3b\omega^2)(2 + \cos 2\Delta\phi))], \end{aligned} \tag{9}$$

$$\begin{aligned} \Delta\dot{\phi}(t) \approx \frac{\omega}{2\pi} \int_t^{t+2\pi/\omega} (\dot{\phi}_L(\tau) - \dot{\phi}_R(\tau)) d\tau \\ = \frac{(r_L^2 + r_R^2)}{8r_Lr_R} [(-4a + (c + 3b\omega^2)(r_L^2 + r_R^2)) \sin \Delta\phi \\ - r_Lr_R(c + 3b\omega^2) \sin 2\Delta\phi]. \end{aligned} \tag{10}$$

Note the appearance of the double angle  $2\Delta\phi$ , which plays a key role in allowing the existence of two stable phases for our system.

We can now determine possible limit cycles by setting the expressions for the time derivatives (8)–(10) equal to zero and solving for  $r_L$ ,  $r_R$ , and  $\Delta\phi$ . Setting the expression (10) equal to zero leads immediately to the critical values  $\Delta\phi = 0$ ,  $\Delta\phi = \pi$ , and

$$\Delta\phi = \cos^{-1} \left( \frac{-4a + (c + 3b\omega^2)(r_L^2 + r_R^2)}{2(c + 3b\omega^2)r_Lr_R} \right).$$

Equating each of the expressions (8) and (9) to zero is algebraically more complicated, but leads to the amplitudes (for the three critical values of  $\Delta\phi$  previously mentioned)

$$|r_L| = |r_R| = \frac{2\sqrt{\alpha - a(1 - \cos \Delta\phi)}}{\sqrt{\gamma + 3\beta\omega^2 - (c + 3b\omega^2)(3 - 4\cos \Delta\phi + \cos 2\Delta\phi)}}.$$

We also find solutions with unequal amplitudes, which is perhaps a bit of a surprise (and has not been previously mentioned in the literature to our knowledge). See Table 1 for a complete listing of the equilibria, the parameter range for which each exists, and stability. We also see that imposing the conditions  $\alpha > 2a$ ,  $\beta > 8b$ , and  $\gamma > 8c$  guarantees the existence of the antiphase solution (#3 in Table 1) for all values of the frequency  $\omega$ . These restrictions are consistent with our assumption of a weak coupling.

Now that we have found the limit cycles, we determine their local stability via an eigenvalue analysis. Equilibrium solution #1 in the table (the zero solution) is an equilibrium of the original system of differential equations, so we can take the usual Jacobian matrix of partial derivatives after rewriting the original second order system

**Table 1.** Equilibria of the system (8)–(10), corresponding to limit cycles of the original system, with conditions under which each exists. We do not list equilibria that duplicate those given here, for example, swapping  $r_L$  and  $r_R$  or changing signs and adjusting  $\Delta\phi$ , or a saddle, depending on the frequency  $\omega$ . The numbering is for convenience in referring to particular limit cycles.

#	Amplitude	Phase difference	Existence Conditions	Stability
1	$r_L = r_R = 0$	—	—	Source
2	$r_L = r_R = 2\sqrt{\frac{\alpha}{\gamma + 3\beta\omega^2}}$	$\Delta\phi = 0$	—	Sink
3	$r_L = r_R = 2\sqrt{\frac{\alpha - 2a}{\gamma + 3\beta\omega^2 - 8(c + 3b\omega^2)}}$	$\Delta\phi = \pi$	$\frac{\alpha - 2a}{\gamma - 8c + 3(\beta - 8b)\omega^2} > 0$	Varies
4	$r_L = r_R = 2\sqrt{\frac{\alpha}{\gamma + 3\beta\omega^2}}$	$\Delta\phi = \cos^{-1}\left(1 - \frac{a(\gamma + 3\beta\omega^2)}{2\alpha(c + 3b\omega^2)}\right)$	$\frac{a}{c + 3b\omega^2} < \frac{4\alpha}{\gamma + 3\beta\omega^2}$	Saddle
5	$r_L = \frac{-\sqrt{\alpha + a} + \sqrt{\alpha\left(1 + \frac{4(c+3b\omega^2)}{\gamma+3\beta\omega^2}\right) - 3a}}{\sqrt{c + \gamma + 3(b + \beta)\omega^2}}$ $r_R = \frac{\sqrt{\alpha + a} + \sqrt{\alpha\left(1 + \frac{4(c+3b\omega^2)}{\gamma+3\beta\omega^2}\right) - 3a}}{\sqrt{c + \gamma + 3(b + \beta)\omega^2}}$	$\Delta\phi = 0$	$\frac{a}{c + 3b\omega^2} < \frac{\alpha}{\gamma + 3\beta\omega^2}$ $\alpha > 8a$ if $\beta > 8b, \gamma > 8c$	Saddle
6	$r_L = \frac{\sqrt{\alpha + a} - \sqrt{\alpha\left(1 + \frac{4(c+3b\omega^2)}{\gamma+3\beta\omega^2}\right) - 3a}}{\sqrt{c + \gamma + 3(b + \beta)\omega^2}}$ $r_R = \frac{\sqrt{\alpha + a} + \sqrt{\alpha\left(1 + \frac{4(c+3b\omega^2)}{\gamma+3\beta\omega^2}\right) - 3a}}{\sqrt{c + \gamma + 3(b + \beta)\omega^2}}$	$\Delta\phi = \pi$	$\frac{3a - \alpha}{4(c + 3b\omega^2)} \leq \frac{\alpha}{\gamma + 3\beta\omega^2} < \frac{a}{c + 3b\omega^2}$	Saddle
7	$r_L = 0, r_R = 2\sqrt{\frac{\alpha - a}{\gamma - c + 3(\beta - b)\omega^2}}$	$\Delta\phi = \pm \frac{\pi}{2}$	—	Saddle



(3)–(4) as a first order system of four equations. This leads to the eigenvalues

$$\lambda_{1,2} = \frac{1}{2}(\alpha \pm \sqrt{\alpha^2 - 4\omega^2}),$$

$$\lambda_{3,4} = \frac{1}{2}(\alpha - 2a \pm \sqrt{(\alpha - 2a)^2 - 4\omega^2}),$$

all four of which have positive real part if  $\alpha > 2a$  and  $\omega \neq 0$ , implying that the equilibrium  $r_L = 0 = r_R$  is a “source” (also called a repeller). That is, once the system is set in motion it does not stop or even asymptotically approach a static state, justifying the label “self-sustaining.”

The local stability of the remaining equilibria (approximate limit cycles of the original system) can be determined by examining the signs of the eigenvalues of the Jacobian matrix

$$J = \frac{\partial(\dot{r}_L, \dot{r}_R, \Delta\dot{\phi})}{\partial(r_L, r_R, \Delta\phi)} \tag{11}$$

evaluated at each equilibrium. An equilibrium is called a source (repelling) if all eigenvalues are positive, a sink (attracting) if all eigenvalues are negative, and a saddle (attracting in some directions, repelling in others) if there are both positive and negative eigenvalues. We hypothesize that a person typically will not move one finger through a significantly larger arc than the other finger (though it would be an interesting experiment to try “asymmetrical twiddling” to see if behavior like that in Figure 5 actually occurs), so we focus our attention on the cases pertinent to our modeling exercise (i.e., those with equal left and right amplitudes; namely #2, #3, and #4 in Table 1).

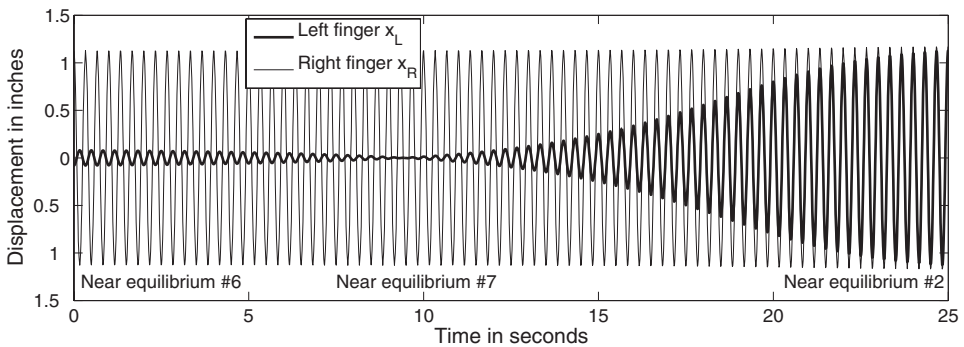


**Figure 5.** The analysis of limit cycles and their local stability does not reveal global behavior of solutions, e.g., the transient behavior of solutions before they finally reach a stable state. Here is an example of coupled oscillators starting near the unstable equilibrium #6. Since this equilibrium is a saddle, the solution remains nearby for many oscillations before veering toward equilibrium #7 (again a saddle), then finally homing in on the sink at equilibrium #2. The parameter values are  $\alpha = 0.5$ ,  $\beta = 0.001$ ,  $\gamma = 0.38$ ,  $a = 0.05$ ,  $b = 0$ ,  $c = 0.036$ , and  $\omega = 6\pi$  (slightly greater than the critical frequency).

The eigenvalues of  $J$  evaluated at equilibrium #2 are

$$\lambda_1 = -2a\pi/\omega,$$

$$\lambda_2 = -2\alpha\pi/\omega,$$

$$\lambda_3 = -2(a + \alpha)\pi/\omega,$$

corresponding to eigenvectors  $[0 \ 0 \ 1]^T$ ,  $[1 \ 1 \ 0]^T$ , and  $[1 \ -1 \ 0]^T$ , respectively. All three eigenvalues are always negative if  $\alpha > 0$  and  $a > 0$ . This solution represents a limit cycle of in-phase oscillations that is called an “attractor” or a “sink,” in the sense that all nearby trajectories approach such a limit cycle. Observe that the eigenvalue  $\lambda_1$ , since it corresponds to eigenvector  $[0 \ 0 \ 1]$ , equals  $\partial(\Delta\dot{\phi})/\partial(\Delta\phi)$  and so controls the rate of convergence of the phase difference  $\Delta\phi$ .

The eigenvalues of  $J$  evaluated at equilibrium #3 are

$$\begin{aligned}\lambda_1 &= -\frac{2\pi}{\omega} \left( \frac{4\alpha(c + 3b\omega^2) - a(\gamma + 3\beta\omega^2)}{\gamma - 8c + 3(\beta - 8b)\omega^2} \right), \\ \lambda_2 &= -\frac{2\pi}{\omega}(\alpha - 2a), \\ \lambda_3 &= -\frac{2\pi}{\omega} \left( \frac{4\alpha(c + 3b\omega^2) + (\alpha - 3a)(\gamma + 3\beta\omega^2)}{\gamma - 8c + 3(\beta - 8b)\omega^2} \right),\end{aligned}$$

corresponding to eigenvectors  $[0 \ 0 \ 1]^T$ ,  $[1 \ 1 \ 0]^T$ , and  $[1 \ -1 \ 0]^T$ , respectively. If  $\alpha \geq 3a$ ,  $\beta > 8b$ , and  $\gamma > 8c$ , then  $\lambda_2$  and  $\lambda_3$  are negative. If we have the further condition that

$$\frac{a}{c + 3b\omega^2} < \frac{4\alpha}{\gamma + 3\beta\omega^2},$$

then  $\lambda_1 < 0$ , in which case this solution represents a stable limit cycle of antiphase oscillations. If

$$\frac{a}{c + 3b\omega^2} > \frac{4\alpha}{\gamma + 3\beta\omega^2},$$

then this limit cycle is an unstable “saddle.” In other words, the stability changes when the frequency increases past the critical value

$$\omega_{cr} = \sqrt{\frac{4\alpha c - a\gamma}{3(a\beta - 4\alpha b)}}. \quad (12)$$

Solutions to the HKB-model can approach a limit cycle by either spiraling in, as shown in graphs (b) and (e) of Figure 4, or via a sequence of segments with slopes approaching 1 or  $-1$ , as shown in graphs (c) and (f). The spiraling occurs when the amplitudes of the two fingers are equal but the phase difference is not at a stable value (not at 0 or  $\pi$ ), in which case the phase difference approaches the stable value very slowly (each cycle takes one second). The sequence of segments occurs when the amplitudes are initially different but the phase difference is at a stable value. Physically, the HKB-model predicts that the fingers approach a stable limit cycle much more slowly than occurs in reality. This slowness also appears in the HKB-model when the frequency is increased past the critical frequency: while our hands rapidly switch from in-phase to antiphase in just two or three cycles, the HKB-model predicts that it takes many cycles, with solutions gradually incrementing the phase difference from 0 to  $\pi$ , indicating a weakness of the model. The addition of noise can speed up the return of the motion to a stable limit cycle following a small perturbation so that the timing is comparable to

that in experimental data [16]. Also note that, as far as the authors know, how human finger motions actually approach the stable limit cycles has not been reported.

Careful examination of (12) reveals the role of various parameters in the HKB-model. If we set either  $\alpha$  or  $a$  equal to zero, then  $\omega_{cr}$  is imaginary and there is no critical frequency triggering a phase transition. If either  $\gamma$  or  $b$  is set equal to zero, then  $\omega_{cr}$  remains well-defined. The parameter  $\gamma$  is not necessary for the phase transition to occur, and its primary role is to ensure that the amplitude does not blow up as  $\omega \rightarrow 0$ . However, the parameter  $b$  plays no important role and could be removed from the model. If we do set  $b = 0$ , then  $\beta$  and  $c$  must both be nonzero in order for  $\omega_{cr}$  to be well-defined. In short, all of the parameters except  $b$  have important roles.

The equilibrium #4 involves a phase difference  $0 < \Delta\phi < \pi$  (somewhere between in-phase and antiphase) and only exists when the antiphase equilibrium #3 is stable (frequency  $\omega < \omega_{cr}$ ). As the frequency increases past the critical value ( $\omega > \omega_{cr}$ ), the antiphase equilibrium become unstable and the equilibrium #4 disappears (in dynamical systems language, a bifurcation occurs at  $\omega = \omega_{cr}$ ). The equilibrium #4, when it exists, is unstable, having two negative eigenvalues and one positive eigenvalue.

**4. PHASE SHIFTS AND ENERGY WELLS.** The HKB-model has an alternate and much simpler form that first appeared in [9] and that has considerable experimental support and is more often cited than the differential equation form (3)–(4). We first explain what this alternate form is and then show how this simpler form can be justified as a proxy for the original model.

The idea is to assume the existence of a function  $V(\Delta\phi; r)$  (called a *potential function*) such that

$$\Delta\dot{\phi} = -\frac{\partial V(\Delta\phi; r)}{\partial \Delta\phi}. \tag{13}$$

One interpretation of the potential function is that it specifies how the system will react given the current phase difference: “My left finger is still ahead of my right finger ( $\Delta\phi > 0$ ) so I should react with  $\Delta\dot{\phi} < 0$  to get the fingers in sync.” To reproduce the four desired properties of the oscillating fingers experiment we need a function with minima at  $\Delta\phi = 0$  and  $\Delta\phi = \pi$  for frequencies below the critical one, and the single minimum at  $\Delta\phi = 0$  above the critical frequency. A simple function that satisfies these constraints is

$$V(\Delta\phi; r) = -A \cos(\Delta\phi) - B \cos(2\Delta\phi), \tag{14}$$

where  $A$  and  $B$  may be functions of amplitude, frequency, and other parameters, and the critical frequency will be associated with  $B/A = 1/4$  (the function  $B/A$  dictates how increasing the frequency affects the relative finger motion; see Figure 6). It is important to note that the amplitude  $r = r_L = r_R$  is assumed to be constant and equal for both fingers for all phase differences, whereas the differential equation model yields different amplitudes for different phase differences. If the coupling is very weak ( $a \ll \alpha$ ,  $b \ll \beta$ , and  $c \ll \gamma$ ), then the amplitudes of equilibria #2, #3, and #4 are quite similar, so it is not unreasonable to simplify the model by assuming a constant amplitude, say, equal to  $2\sqrt{\alpha/(\gamma + 3\beta\omega^2)}$ .

In order to link the differential equation form of the HKB-model given by (3)–(4) to this potential function form, we examine the role of  $\partial(\Delta\dot{\phi})/\partial(\Delta\phi)$  in the eigenvalue analysis of the previous section. We wish to link the eigenvalue governing the stability of the phases to the potential function  $V$ . The Jacobian matrix  $J$  as de-

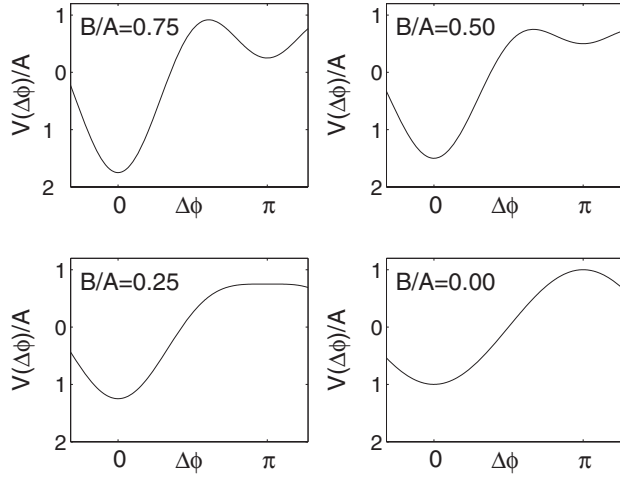


**Figure 6.** Graphs of the potential function  $V(\Delta\phi) = -A \cos \Delta\phi - B \cos 2\Delta\phi$  that governs the phase difference between the two fingers. Both in-phase ( $\Delta\phi = 0$ ) and antiphase ( $\Delta\phi = \pi$ ) bimanual motion are stable for  $B/A > 0.25$  (both correspond to minima of  $V$ ), but only the in-phase is stable for  $B/A < 0.25$  (antiphase now corresponds to a maximum of  $V$ ).

defined in (11) and evaluated at either of the equilibria #2 and #3 has an eigenvalue  $\lambda_1 = \partial(\Delta\dot{\phi})/\partial(\Delta\phi)$  corresponding to eigenvector  $[0 \ 0 \ 1]^T$ . The sign of this eigenvalue determines the stability of the phase difference (that is, whether in-phase and antiphase motions are stable). The eigenvalues  $\lambda_2$  and  $\lambda_3$  correspond to the eigenvectors  $[1 \ 1 \ 0]^T$  and  $[1 \ -1 \ 0]^T$  and so govern the amplitudes  $r_L$  and  $r_R$  near each equilibrium. These eigenvalues are both negative if  $\alpha \geq 3a$ , ensuring that, as the frequency  $\omega$  varies, the amplitudes remain very stable while the phase difference  $\phi = \pi$  can possibly lose stability.

We can also argue for the validity of (13) in the context of our eigenvalue analysis. We want minima of  $V$  (which satisfy  $\partial^2 V/\partial(\Delta\phi)^2 > 0$ ) to correspond to stable equilibria (where  $\partial(\Delta\dot{\phi})/\partial(\Delta\phi) < 0$ ), and so we write

$$\frac{\partial(\Delta\dot{\phi})}{\partial(\Delta\phi)} = -\frac{\partial^2 V}{\partial(\Delta\phi)^2}. \quad (15)$$

Equation (15) associates the sign of the eigenvalue  $\partial(\Delta\dot{\phi})/\partial(\Delta\phi)$  with the concavity of the potential function  $V(\Delta\phi; r)$ . Integrating (15) with respect to  $\Delta\phi$  leads to (13). In order to determine the potential function  $V$  for the HKB-model, substitute into (13) the expression for  $\Delta\dot{\phi}$  given in (10), taking  $r = r_L = r_R$ , and then integrate both sides with respect to  $\Delta\phi$ . This yields the following potential function:

$$V(\Delta\phi; r) = (-a + (3b\omega^2 + c)r^2/2) \cos(\Delta\phi) - \frac{1}{8}(3b\omega^2 + c)r^2 \cos(2\Delta\phi). \quad (16)$$

We see that  $V$  has the desired form (14), with  $A = a - (3b\omega^2 + c)r^2/2$  and  $B = (3b\omega^2 + c)r^2/8$ .

The dynamical system generated by (13) and (16) and the differential equation system (3)–(4) exhibit similar dynamics in the sense that the minima of  $V$  correspond to stable limit cycles for  $\Delta\phi = 0$  and  $\Delta\phi = \pi$ . Also, the minimum of  $V$  at  $\Delta\phi = \pi$  changes to a maximum if the frequency increases past the critical value, while simultaneously the maximum at  $\Delta\phi = \cos^{-1}(-A/4B)$  disappears, in parallel with the bifurcation (signaling a phase transition) that occurs in (3)–(4). However, this poten-

tial function form of the HKB-model is *not* equivalent to the differential equation form. The dynamical system (13)–(14) is one-dimensional (in  $\Delta\phi$  only) and the antiphase equilibrium is a source for  $\omega > \omega_{cr}$ , whereas the ODEs (3)–(4) lead to a three-dimensional dynamical system (in  $r_L, r_R,$  and  $\Delta\phi$ ) in which the antiphase equilibrium becomes a saddle. Also, we have played rather fast and loose with the eigenvalues of the linearization of the approximated system (8)–(10) in order to generate a potential function with the desired qualitative dynamics.<sup>2</sup>

**5. CLOSING REMARKS.** At first glance, the HKB-model may seem to be contrived in the sense that, while it reproduces observed phenomena reasonably well, it is not derived from first principles, as these are currently uncertain. The model is not completely ad hoc, however, and should not be immediately dismissed (see, for example, the in-depth discussions of various approaches to constructing nonlinear dynamical models based on experimental data in the context of human motion in [1], [3], or [7]). This model is a vital, early step in a broader research effort aimed at uncovering fundamental features of pattern formation at all scales, from clusters of neurons to parts of the body to groups of people. The incredible complexity of these dynamical systems, compounded by our current paucity of knowledge, means that any attempt to create relatively accurate quantitative models is unlikely to lead to an increase in an understanding of the underlying principles that govern such systems. On the other hand, focusing attention on a relatively simple, representative phenomenon, like the one described in this article, and then developing a mathematical model that reproduces key features, can lead to greater insight, which, after all, is the principle goal of modeling.

The HKB-model has been successful in this sense: it has indeed led to important insights about coordinated movement. As described earlier, analysis of the HKB-model supports the hypothesis that, in order for a system to have both multiple states and the possibility of switching between them, it must be nonlinear with nonlinear coupling. We saw that the critical frequency  $\omega_{cr}$  emerges only if we have a nonlinear damping expression  $-\alpha\dot{x} + \beta\dot{x}^3 + \gamma x^2\dot{x}$  in the description of an individual oscillator, plus a nonlinear coupling function  $-a(\dot{x}_L - \dot{x}_R) + c(x_L - x_R)^2(\dot{x}_L - \dot{x}_R)$ . This critical result reveals that nonlinearity lies at the heart of these systems and is the key to producing flexible but stable behavior (i.e., multiple stable states with the ability to switch between them by changing a key parameter). At a higher level, not only has the exploration of the HKB-model led to much fruitful discussion, further experiments, and the discovery of interesting properties of the human neuromuscular system, but it has also helped pave the way to the idea of self-organization by dynamical systems within the human nervous system as well as within human society (see [12], particularly chapter 4).

It must be recognized, however, that there are some serious weaknesses in the original HKB-model. The model does not allow other possible stable phase differences, it does not include the role of perception in coordination, and the predicted approaches to stable states and to switching between stable states are much slower than observed. Moreover, solutions can be pulled toward possibly nonphysical states, such as the near-

---

<sup>2</sup>To analyze the approximate system more rigorously, one could note that the stable invariant manifold for the antiphase equilibrium is homeomorphic to the  $r_L r_R$ -plane. The unstable invariant manifold is homeomorphic to the line  $\phi = \pi$  if  $\omega > \omega_{cr}$ , but at  $\omega = \omega_{cr}$  a center manifold replaces the unstable manifold and is tangent to the line  $\phi = \pi$  (invoking the Hartman-Grobman and center manifold theorems, see [5, p. 31]). For the purposes of understanding qualitative dynamics, this approach involves extra work for little or no benefit to the modeling goals. The approach taken here of disregarding what happens to the amplitude and focusing on the critical eigenvalue that governs  $\Delta\phi$  satisfies our needs.

zero amplitude seen in Figure 5, before finally approaching a stable limit cycle. Finally, although the HKB differential equation model only matches local stability properties, we would ideally like the model to have global stability properties that match physical behavior (the potential function form somewhat ameliorates this problem). Extensions to the model have addressed some of these issues.

The HKB-model can serve as a gateway to a deeper understanding of more complex phenomena such as gait changes in horses, insects, and even millipedes. For example, [6] and [8] show, using symmetry arguments, that an appropriate coupling of  $2n$  differential equation cells leads to accurate predictions of stable gaits for a creature with  $n$  legs. Interestingly, some researchers [2] have attempted to improve the HKB-model via two pairs of oscillators (one coupled pair of “neural” oscillators that both couple to an oscillator representing a finger), in a curious parallel to the  $2n$  cells developed by Golubitsky and coworkers. These models hint at how our neuromuscular systems might work, although no clear consensus has emerged on this issue. What *is* clear is that there remain many opportunities for interesting modeling to be done in this area.

## REFERENCES

1. P. J. Beek and W. J. Beek, Tools for constructing dynamical models of rhythmic movement, *Human Movement Science* **7** (1988) 301–342.
2. P. J. Beek, C. E. Peper, and A. Daffertshofer, Modeling rhythmic interlimb coordination: Beyond the Haken-Kelso-Bunz model, *Brain and Cognition* **48** (2002) 149–165.
3. P. J. Beek, W. E. I. Rikkert, and P. C. W. van Wieringen, Limit cycle properties of rhythmic forearm movements, *J. Exper. Psych.: Human Perception and Performance* **22** (1996) 1077–1093.
4. G. P. Bingham, A perceptually driven dynamical model of bimanual rhythmic movement (and phase perception), *Ecol. Psych.* **16** (2004) 45–53.
5. C. Chicone, *Ordinary Differential Equations with Applications*, Texts in Applied Mathematics, no. 34, Springer-Verlag, New York, 1999.
6. P.-L. Buono and M. Golubitsky, Models of central pattern generators for quadruped locomotion. I. Primary gaits, *J. Math. Biol.* **42** (2001) 291–326.
7. T. Eisenhammer, A. Hübler, N. Packard, and J. A. S. Kelso, Modeling experimental time series with ordinary differential equations, *Biol. Cybernet.* **65** (1991) 107–112.
8. M. Golubitsky, I. Stewart, P.-L. Buono, and J. J. Collins, A modular network for legged locomotion, *Phys. D* **115** (1998) 56–72.
9. H. Haken, J. A. S. Kelso, and H. Bunz, A theoretical model of phase transitions in human hand movements, *Biol. Cybernet.* **51** (1985) 347–356.
10. B. A. Kay, J. A. S. Kelso, E. L. Saltzman, and G. Schöner, Space-time behavior of single and bimanual rhythmical movements: Data and limit cycle model, *J. Exper. Psych.: Human Perception and Performance* **13** (1987) 178–192.
11. J. A. S. Kelso, On the oscillatory basis of movement, *Bull. Psychonomic Soc.* **18** (1981) 63.
12. ———, *Dynamic Patterns: The Self-Organization of Brain and Behavior*, MIT Press, Cambridge, 1997.
13. J. A. S. Kelso, G. Schöner, J. P. Scholz, and H. Haken, Phase-locked modes, phase transitions and component oscillators in biological motion, *Phys. Scripta* **35** (1987) 79–87.
14. N. Minorsky, *Nonlinear Oscillations*, Van Nostrand, Princeton, 1962.
15. R. C. Schmidt, C. Carello, and M. T. Turvey, Phase transitions and critical fluctuations in the visual coordination of rhythmic movements between people, *J. Exper. Psych.: Human Perception and Performance* **16** (1990) 227–247.
16. G. Schöner, H. Haken, and J. A. S. Kelso, A stochastic theory of phase transitions in human hand movement, *Biol. Cybernet.* **53** (1986) 247–257.

**TANYA L. LEISE**, who received her Ph.D. from Texas A&M in 1998, is a visiting assistant professor of mathematics at Amherst College. While her previous research focused on the dynamics of accelerating cracks in elastic and viscoelastic media, she has recently developed an interest in the dynamics of coupled nonlinear oscillators in the contexts of rhythmic motion and chronobiology. She is currently most interested in adjusting the circadian rhythm of her 5-year-old daughter, that is, in getting her to go to bed at a reasonable hour.

*Department of Mathematics and Computer Science, Amherst College, Amherst, MA 01002*  
*tleise@amherst.edu*

**ANDREW L. COHEN** received a M.Sc. in Computer Science from Texas A&M University in 1996 and a Ph.D. in Psychology and Cognitive Science from Indiana University in 2002. He is currently an assistant professor of psychology at the University of Massachusetts, Amherst. His research interests lie in investigating the building blocks, or features, that underlie perception and exploring how multiple features are combined to determine higher-level cognitive decisions in tasks of perceptual classification, recognition memory, judgment, and identification.

*Department of Psychology, University of Massachusetts-Amherst, Amherst, MA 01003*  
*acohen@psych.umass.edu*

### **A Mean Value Theorem for One-Sided Derivatives**

**Theorem.** *Suppose that  $f$  is continuous on  $[a, b]$  and the right derivative  $D_+f(x)$  is defined for all  $x \in (a, b)$ . Then there are numbers  $p, q \in (a, b)$  such that*

$$D_+f(p) \geq \frac{f(b) - f(a)}{b - a} \geq D_+f(q).$$

*Proof.* Suppose first that  $f(a) = f(b) = 0$ . If  $f$  is a constant function then the conclusion is clear. Now suppose that  $f(x) > 0$  for some  $x \in (a, b)$ . Then the maximum value of  $f$  occurs at some number  $q \in (a, b)$  with  $f(q) > 0$ . Now choose  $p \in (a, q)$  such that  $f(p) = f(q)/2$  and  $f(x) > f(q)/2$  for all  $x \in (p, q)$ . Clearly  $D_+f(p) \geq 0 \geq D_+f(q)$ . Similar reasoning can be used if  $f(x) < 0$  for some  $x \in (a, b)$ .

Finally, the theorem for general  $f$  can be deduced from the case we have dealt with by subtracting a linear function from  $f$ . ■

Of course, a similar theorem holds for left derivatives. For an application of these theorems, see p. 39.

—Submitted by Donald Minassian, Butler University, Indianapolis, IN